Parametric spectral correlations of disordered systems in the Fourier domain

Italo Guarneri,[1,2] Karol Życzkowski,[1,3] Jakub Zakrzewski,[3,4] Luca Molinari,[5] and Giulio Casati[1,6]

[1]*Università di Milano, sede di Como, via Lucini 3, 22100 Como, Italy*

[2]*Istituto Nazionale di Fisica Nucleare, Sezione di Pavia, Via Bassi 6, 27100 Pavia, Italy*

[3]*Instytut Fizyki Uniwersytetu Jagiellońskiego, ul. Reymonta 4, 30-059 Kraków, Poland*

[4]*Laboratoire Kastler Brossel, Université Pierre et Marie Curie, T12, E1, 4 place Jussieu, 75272 Paris Cedex 05, France*

[5]*Dipartimento di Fisica, Università di Milano, Via Celoria 16, Milano, Italy*

[6]*Istituto Nazionale di Fisica Nucleare, Sezione di Milano, via Celoria 16, Milano, Italy*

A Fourier analysis of parametric level dynamics for random matrices periodically depending on a phase is developed. We demonstrate both theoretically and numerically that under very general conditions the correlation $C(\varphi)$ of level velocities is singular at $\varphi=0$ for any symmetry class; the singularity is revealed by algebraic tails in Fourier transforms, and is milder, the stronger the level repulsion in the chosen ensemble. The singularity is strictly connected with the divergence of the second moments of level derivatives of appropriate order, and its type is specified to leading terms for Gaussian, stationary ensembles of orthogonal (GOE), unitary (GUE), and symplectic (GSE) types, and for the Gaussian ensemble of periodic banded random matrices, in which a breaking of symmetry occurs. In the latter case, we examine the behavior of correlations in the diffusive regime and in the localized one as well, finding a singularity like that of pure GUE cases. In all the considered ensembles we study the statistics of the Fourier coefficients of eigenvalues, which are Gaussian distributed for low harmonics, but not for high ones, and the distribution of kinetic energies.

PACS number(s): 05.45.+b

I. INTRODUCTION

In this paper, we shall be concerned with spectral properties of random matrices $H(\varphi)$, periodically depending on a phase $\varphi \in [0, 2\pi]$. Random matrices [1] are often used to describe statistical properties of disordered mesoscopic systems [2–4]. In particular, random matrices parametrically dependent on a phase are used as models for conduction in small metallic rings threaded by an Ahronov-Bohm flux $\varphi h/e$, and great attention is being devoted to the dependence of their eigenvalues $e_i(\varphi)$ on the phase φ [5–10]. Objects of particular interest are the statistics of level slopes $e_i'(\varphi)$ (also called level velocities; a prime denotes a derivative with respect to φ), of level curvatures $e_i''(\varphi)$, and velocity-velocity autocorrelations

$$C(\varphi) := \frac{1}{2\pi\Delta^2} \int_0^{2\pi} \langle e_i'(\varphi')e_i'(\varphi'+\varphi)\rangle d\varphi'$$

$$= \frac{1}{\Delta^2} \overline{\langle e_i'(\varphi')e_i'(\varphi'+\varphi)\rangle} , \qquad (1.1)$$

where $\langle\ \rangle$ denotes ensemble averaging, the bar denotes phase averaging, and Δ is the average level spacing.

Autocorrelation functions that are closely related to (1.1) (at least insofar as a single-particle description is valid) are also accessible to laboratory experiments on quantum dots [11].

To the extent that random matrices can be taken as models for the Hamiltonians of quantum systems that become chaotic in the classical limit, the identification of "universal" properties of parametric level dynamics is also relevant for quantum chaology [12]. In that case,

the phase φ represents any external parameter that determines the spectrum. The motion of levels as functions of φ may be thought of as a dynamics of fictitious particles (with positions e_i), with φ playing the role of "time."

In a series of papers, Altshuler and co-workers [7] have shown that for disordered metallic systems the parametric statistics are, in fact, universal, after rescaling the levels to unit mean spacing and also rescaling the parameter φ as $X = \pi\varphi\sqrt{c}$, with $c = C(0)$ denoting the mean squared velocity of energy levels. Therefore, the only two system-specific parameters are Δ and c; the latter has the meaning of twice the average kinetic energy of the level moving in the time φ. An example of such a parametric universality has been discussed earlier in studies of level curvatures [13–15].

In particular, the theory [7] leads to a remarkable scaling property of the velocity-velocity autocorrelation (1.1):

$$C(\varphi) \approx c\Phi(\pi\varphi\sqrt{c}) = c\Phi(X) . \qquad (1.2)$$

In Eq. (1.2), $\Phi(\ )$ is a universal function, only dependent on the general symmetry properties of the chosen matrix ensembles. Determining the shape of this universal function is manifestly an important task. At large X, the behavior $\Phi(X) \sim -X^{-2}$ was theoretically predicted [7,5,6] and numerically tested [16]; instead, the small X behavior appears to critically depend on the chosen ensemble. Explicit expressions have been obtained [7] for a closely related [but distinct from $C(\varphi)$] autocorrelation function at fixed energy. The resulting expressions are valid for homogeneous ensembles only, in which the symmetry class of the random matrix is independent of φ, and are quite complicated (for the orthogonal ensemble a

triple integral with regularization is required). A global approximation for $\Phi(X)$ has been proposed [16]. For the case of a classically chaotic system subject to a Aharonov-Bohm flux, Berry and Keating [17] have recently obtained a semiclassical approximation for $C(\varphi)$ having the form of an everywhere analytic function of φ.

In this paper, we shall investigate correlations (1.1) in various ensembles of phase-dependent random matrices, using Fourier analysis, which is particularly well suited to this purpose, because of periodicity, and also because the singularities of $C(\varphi)$ are easily detected by this technique. We shall consider the case of homogeneous Gaussian ensembles, with orthogonal (GOE), unitary (GUE), and symplectic (GSE) symmetry, and also the physically important situation, in which the time-reversal symmetry is broken and a transition from GOE to GUE occurs while switching on the "Aharonov-Bohm flux" φ. The latter case will be analyzed on the ensemble of periodic band random matrices (PBRM) [8], which exhibits the three characteristic regimes of conduction in disordered solids, namely, the localized, the (proper) diffusive, and the ballistic one.

A general theoretical approach to the Fourier analysis of spectral correlations is developed in Sec. II, where it is shown that under very general conditions, $C(\varphi)$ must have a singularity at $\varphi=0$, signaled by an algebraic tail in its Fourier transform. This result is valid even in cases (such as homogeneous GUE, GSE) which were hitherto believed to be singularity free. The singularity is, however, milder, the stronger the level repulsion in the considered ensemble. We determine its exact type for various symmetry classes. For the homogeneous cases our predictions are confirmed by numerical results, presented in Sec. III and by the exact solution for matrices of rank 2, presented in the Appendix. The model of PBRM corresponding to the Aharonov-Bohm case is analyzed in Sec. IV. We present theoretical arguments and numerical results supporting the thesis that for this case, the behavior of the correlation function at $\varphi=0$ is similar to the one observed in the homogeneous GUE case, and we compare our data to other theoretical predictions. Furthermore, we present distributions of avoided crossings for PBRM, which are deeply related to the properties of the velocity correlation function, and briefly discuss the modifications of the correlation function that occur on moving towards the localized regime.

Further applications of Fourier analysis presented in this paper include the statistics of various quantities. Among these, the Fourier amplitudes of level velocities (currents), which are found to be Gaussian for low harmonics but not for high ones, and the mean squared current, which appears to follow a χ^2 distribution with an appropriate number of degrees of freedom. Finally, we discuss the moments of level derivatives of order k with respect to phase φ and find them either to diverge (if k is not small enough) or to be directly related, via the scaling law, to the average kinetic energy of levels.

II. FOURIER ANALYSIS

In full generality, by a periodic random matrix (PRM) we mean a random matrix $H(\varphi)$ periodically depending on a phase φ; more precisely, a matrix-valued, periodic, stochastic process, taking values in a class of matrices having a definite symmetry (symmetric, complex-Hermitian, symplectic), which is not necessarily the same for all values of φ. An ensemble of PRM is not an ensemble of matrices, but an ensemble of *trajectories* $H(\varphi)$ in a space of matrices; every such trajectory will be called a realization of the ensemble. In this paper, we shall consider stationary ensembles, such that their statistics is invariant under translations $\text{mod}(2\pi)$ of the phase φ, and nonstationary ones as well. Although the numerical results described in this paper were obtained for some very specific, well-defined ensembles, the argument to be presently described is applicable under rather general assumptions, hence to a much broader class of ensembles.

Our first assumption is that with probability one, the trajectory $H(\varphi)$ is an entire function of φ. On the strength of this assumption, the eigenvalues $e(\varphi)$ of almost any realization $H(\varphi)$ are analytic functions of φ, and their behavior in a neighborhood of any point φ in $[0,2\pi]$ can be described by analytic perturbation theory. The corresponding convergence radii, however, are realization dependent. If they can become arbitrarily small in a statistically significant fraction of the ensemble, perturbative methods will not be applicable to the calculation of certain statistical averages. This is precisely the situation we are going to discuss below.

Given a realization $H(\varphi)$, any eigenvalue $e(\varphi)$ can be expanded in a Fourier series. The Fourier expansions we shall use are

$$e(\varphi)=\sum_{-\infty}^{+\infty} a_n e^{in\varphi}, \quad C(\varphi)=\sum_{-\infty}^{+\infty} c_n e^{in\varphi}, \qquad (2.1)$$

where $a_n=a_{-n}^*$ and, on account of Eq. (1.1), $c_n=n^2\Delta^{-2}\langle |a_n|^2\rangle$. The statistical average $\langle \ \rangle$ is meant as an average over all the eigenvalues lying in a selected energy range (in the following we drop a subscript i denoting a given level in e_i), followed by an average over all realizations in some ensemble. Because $C(\varphi)$ is a correlation function, it must be even, $C(\varphi)=C(2\pi-\varphi)$. From (2.1) it follows that

$$c=C(0)=\sum_{-\infty}^{+\infty} c_n .$$

If, in the chosen ensemble, a scaling law of the form (1.2) holds, then, at $c\gg1$,

$$c_n \approx \sqrt{c}\, P\left[\frac{n}{\sqrt{c}}\right] , \qquad (2.2)$$

with $P(t)$ a function related to the Fourier transform of $\Phi(X)$ [Eq. (1.2)],

$$P(t)=(2\pi^2)^{-1}\int \Phi(X)e^{-itX/\pi}dX . \qquad (2.3)$$

It follows that $P(t)$ defines a probability distribution on the real line, with (not necessarily finite) moments $A^{(\alpha)}=\langle |t^\alpha|\rangle$. In particular, the width of the Fourier spectrum is measured by

$$\langle |n| \rangle := \frac{\sum\limits_{-\infty}^{+\infty} |n| c_n}{\sum\limits_{-\infty}^{+\infty} c_n} \approx \sqrt{c} \int |t| P(t) dt = A^{(1)} \sqrt{c} \ . \qquad (2.4)$$

Even moments are related in an obvious way to derivatives of Φ at the origin,

$$\Phi^{(2k)}(0) = (-1)^k \pi^{-2k} A^{(2k)} \ . \qquad (2.5)$$

In ensembles for which the scaling theory [7] is valid, the functions Φ and P and the constants $A^{(\alpha)}$ depend on the universality class only, which will be occasionally specified in the following by a suffix β (as, e.g., in Φ_β), with $\beta = 1, 2, 4$ for the GOE, GUE, and GSE universality classes, respectively; or by the suffix AB in the symmetry-breaking GOE-GUE case. Equations (2.2) and (2.4) provide a way to check the scaling hypothesis in the Fourier domain. For the specific ensembles considered in the following sections, they were indeed confirmed by our numerical computations, to be discussed later.

Following our previous assumption, $H(\varphi)$ can be analytically continued to the whole complex φ plane. Any eigenvalue $e(\varphi)$ is an analytic function of the complex variable φ, except for branch points (BP's) $z_j = \varphi_{0j} + i\gamma_j$ corresponding to complex level crossings [18]. The index j labels the BP's, $j = 1, \ldots, \mathcal{N}$, with $\mathcal{N}$ the total number of BP's exhibited by the given level as a function of φ in the complex domain. Since $e(\varphi)$ is real at real φ, these BP's are distributed symmetrically with respect to the real axis, but none of them falls on the real axis itself [33]. Therefore, given a realization $H(\varphi)$, the function $e(\varphi)$ is analytic inside a strip of halfwidth Γ around the real axis, Γ being the smallest of the $|\gamma_j|$. In order to estimate the complex Fourier coefficients

$$a_n = \frac{1}{2\pi} \int_0^{2\pi} e^{-in\varphi} e(\varphi) d\varphi \ ,$$

with $n < 0$ we use the multiple path illustrated in Fig. 1. In the following we assume $n < 0$ (if $n > 0$ the path must be reflected with respect to the real axis; the corresponding analysis differs from the following one by obvious modifications). In this way,

$$a_n = \sum_{j=1}^{\mathcal{N}} I_j \ , \qquad (2.6)$$

where I_j is the complex contribution of the jth branch line,

$$I_j = \frac{e^{-inz_j}}{2\pi} \int_0^\infty dx \, e^{-|n|x} \delta e_j(x) \ , \qquad (2.7)$$

and $\delta e_j(x)$ is the jump of $e(\varphi)$ across the jth branch cut, at the point $\varphi = z_j + ix$. The behavior of the Laplace in-
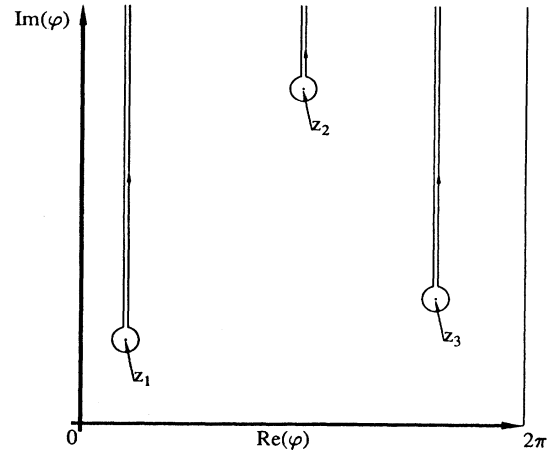

FIG. 1. Multiple complex path used in the calculation of the Fourier amplitudes a_n with $n < 0$. Three branch points are shown.

tegral (2.7) at large n is determined by the behavior of $\delta e_j(x)$ close to the BP, as we shall presently discuss. We concentrate on BP's with $\gamma_j \ll 1$, whose contribution will dominate at large n. We shall consider simple BP's only; in other words, we shall attribute zero statistical weight to crossings involving more than two levels. If a realization $H(\varphi)$ (φ complex) is thought of as a two-(real)parameters family of matrices, then generically such a family will not contain matrices exhibiting higher-order degeneracies, because, multiple level crossings cannot generically be achieved by varying just two real parameters. Therefore, the assumption we need to justify our neglecting higher-order BP's is just that such nongeneric realizations $H(\varphi)$ have zero probability; this is a smoothness assumption on the statistical distribution of the ensemble, which appears fairly general.

For φ real and close to φ_{0j} the considered level is undergoing a narrow avoided crossing. It is, in fact, close to degenerate with a different level, the two eigenvalues being approximately,

$$e_\pm(\varphi) \approx E_j \pm h_j \sqrt{\gamma_j^2 + (\varphi - \varphi_{0j})^2} \ . \qquad (2.8)$$

Carrying this to complex φ we get, for φ close to z_j, $\delta e_j(\varphi) \approx 2h_j \sqrt{\gamma_j x}$. Substituting into (2.7), and using known estimates for Laplace integrals [19], we obtain

$$I_j \sim \frac{h_j}{\pi} \sqrt{\gamma_j} |n|^{-3/2} e^{-inz_j} \ . \qquad (2.9)$$

We now introduce the single-level velocity correlation function (CF),

$$R(\varphi) := \Delta^{-2} \overline{e'(\varphi')e'(\varphi'+\varphi)} = \sum_{n=-\infty}^{+\infty} r_n e^{in\varphi} \ , \qquad (2.10)$$

(the bar denoting average over φ'), which depends on the chosen eigenvalue, and on the realization as well. This function is connected to the original CF by $C(\varphi) = \langle R(\varphi) \rangle$, and $c_n = \langle r_n \rangle$. From (2.9) we obtain

$$r_n = \Delta^{-2} n^2 |a_n|^2 \sim \frac{\Gamma}{|n|} e^{-2|n|\Gamma} . \qquad (2.11)$$

Thus, prior to ensemble averaging, $R(\varphi)$ has an exponentially decaying Fourier expansion, and is, therefore, analytic in a strip of halfwidth 2Γ. From (2.11) it actually follows that $R(\varphi)$ has logarithmic singularities at $\varphi = \pm 2i\Gamma + 2k\pi$, with leading terms $\Gamma \ln(\varphi \pm 2i\Gamma + 2k\pi)$. Therefore, for real φ close to 0, $R(\varphi)$ behaves like $\Gamma \ln(\varphi^2 + 4\Gamma^2)$. On averaging over the matrix ensemble, arbitrarily small Γ come into play, that is, the logarithmic singularities of $R(\varphi)$ come arbitrarily close to the real axis. As a result, $C(\varphi)$ will not be analytic at $\varphi = 0$ anymore; the type of singularity will depend on the statistical weight that is given to small Γ in the chosen ensemble. Actually, a standard probability-theoretic argument, quite independent of the above elaborations, shows that in order for $C(\varphi)$ to be analytic, too small Γ must not be allowed at all.

In fact, if we assume $C(\varphi)$ to be analytic, then, being also periodic, it must have an analyticity strip of (strictly) nonzero width $2L > 0$. Then the coefficients c_n must satisfy

$$c_n < K_{L'} e^{-2L'|n|} ,$$

for all $L' < L$ (with appropriate constants $K_{L'}$). Since $c_n = n^2 \Delta^{-2} \langle |a_n|^2 \rangle$, the probability $p_n(L'')$ that $|a_n|$ be larger than $e^{-L''|n|}$ will satisfy the Chebyshev inequality [20],

$$p_n(L'') < c_n n^{-2} \Delta^2 e^{2L''|n|} < K_{L'} \Delta^2 e^{-2(L'-L'')|n|} .$$

Therefore, $\sum_n p_n(L'') < +\infty$ as soon as $L'' < L$. Then the Borel-Cantelli lemma of probability theory [21] ensures that, with probability one, all but finitely many of the coefficients a_n satisfy $|a_n| < e^{-L''|n|}$ for any $L'' < L$. In turn, this implies that $e(\varphi)$ is analytic in a strip of width L with probability one; that is, the probability of a branch point lying closer than L to the real axis is zero. Therefore, in order to get an analytic $C(\varphi)$ everywhere, the ensemble must be such that the distribution of the imaginary part of BP's has a finite gap. Since the latter distribution is clearly related to the distribution of the widths of avoided crossings, this appears to be rather an exceptional situation.

In order to get more precise information about the nature of the singularities of $C(\varphi)$, a knowledge of the statistical distribution of the BP's is needed, which cannot be obtained under the general assumptions made up to now. We shall then assume that this distribution is described by a density $p(\gamma, \varphi_0)$, and also that different BP's give uncorrelated contributions. Furthermore, in the rest of this section, we shall restrict ourselves to stationary ensembles, such that all statistical properties are independent of φ; explicit examples will be given in the next section. In such cases, we can assume statistical independence of φ_0 and γ, and a uniform distribution for the former. In other words, $p(\gamma, \varphi_0) = f(\gamma)/(2\pi)$. Then, from Eqs. (2.6) and (2.9) we obtain

$$c_n \sim \frac{\langle h^2 \rangle \mathcal{N}}{\pi \Delta^2 |n|} \int_0^\infty d\gamma \, \gamma e^{-2|n|\gamma} f(\gamma) . \qquad (2.12)$$

In order to assess how this expression scales with c, we first notice from (2.8) that the quantity h sets the scale for the level velocity close to the avoided crossing. Therefore, we assume $\langle h^2/\Delta^2 \rangle$ to scale as the variance of the rescaled level velocity, that is, as $c = C(0) = \sum c_n$. At the same time, $h\gamma$ is the width of the avoided crossing and this identifies the scale of γ with that of $\Delta/h \sim c^{-1/2}$. On such grounds, setting $\gamma = xc^{-1/2}$, we expect

$$f(\gamma) = c^{1/2} F(\gamma c^{1/2}) ,$$

with $F(x)$ a scale-independent distribution. Substituting this into (2.12) we obtain

$$c_n \sim \alpha \mathcal{N} \frac{\sqrt{c}}{|n|} \int_0^\infty dx \, F(x) x e^{-2x|n|/\sqrt{c}} , \qquad (2.13)$$

(in the rest of this section, α will denote undetermined numerical factors). In order to estimate $\mathcal{N}$, we identify its order of magnitude with that of the number of avoided crossings experienced by $e(\varphi)$ as φ varies between 0 and 2π, which has been found to be proportional to $\sqrt{c}$ using two different approaches [22,24]. We are thus finally led to

$$c_n \sim \alpha \frac{c}{|n|} \int_0^\infty dx \, F(x) x e^{-2x|n|/\sqrt{c}} . \qquad (2.14)$$

This formula has a number of implications. In the first place, it is exactly of the form (2.2); the above argument has led us to an independent confirmation of the scaling law at $|n| \gg \sqrt{c}$. Second, it yields an asymptotic estimate for the universal function $P(t)$ at large t,

$$P(t) \sim \frac{\alpha}{t} \int_0^\infty dx \, F(x) x e^{-2tx} . \qquad (2.15)$$

It does not appear legitimate, however, to use formula (2.14) outside the asymptotic regime $|n| \gg \sqrt{c}$, because of the underlying asymptotic estimate (2.9).

To proceed further, we need to specify $F(x)$, or at least its behavior at $x \ll 1$, which determines the asymptotics of (2.14) at large n. The variable x is, apart from rescaling, the same as γ, which is in turn closely related to the width of an avoided crossing. For the case of Gaussian ensembles, the statistics of the latter quantity has been studied in [22–24], where the probability of small avoided crossings of size ϵ was found to scale as $\epsilon^{\beta-1}$, with β the repulsion parameter characteristic of the given ensemble. This result is actually very general. According to (2.8), the probability of a small level spacing less than ϵ, which scales as $\epsilon^{\beta+1}$, is also proportional to the probability of getting a BP inside a small circle of radius ϵ in the complex φ plane. The latter probability scales as $\epsilon \int_0^\epsilon f \, d\gamma$, whence $f(\epsilon) \sim \epsilon^{\beta-1}$.

Our last assumption will be that level repulsion in our (stationary) ensemble is ruled by a repulsion exponent β. Then, substituting $F(x) \sim x^{\beta-1}$ (at small x) into Eq. (2.15) we finally get

$$P(t) \sim \alpha t^{-2-\beta} , \qquad (2.16)$$

which is the main result of this section. It implies that in no stationary ensemble can $C_\beta(\varphi)$ be a smooth function at $\varphi = 0$, because its $(\beta+1)$th derivative must have a singu-

larity there. It should be noted that the asymptotic behavior $c_n \sim n^{-2-\beta}$, which leads to this conclusion, directly follows from Eq. (2.12) and from the fact that the probability of small γ scales as $\gamma^{\beta-1}$, independently of the scaling considerations following Eq. (2.12).

The nature of the singularity associated with the behavior (2.16) now follows, either from known results in Fourier analysis, or, more directly, from statistically averaging the previously described small-φ behavior of $R(\varphi)$. The resulting small-φ expansions for the cases $\beta=1,2,4$, written in terms of the scaled variable $X=\pi\varphi\sqrt{c}$, are (up to leading terms only)

$$C_1(\varphi)/c \sim 1 + b_1 X^2 \ln|X| ,$$

$$C_2(\varphi)/c \sim 1 - b_2 X^2 + b_3 |X^3| , \qquad (2.17)$$

$$C_4(\varphi)/c \sim 1 - b_4 X^2 + b_5 X^4 + b_6 |X^5| .$$

Some of the coefficients b_n will be specified later, for specific choices of the PRM ensemble.

Scaling and level derivatives

The statistics of BP's not only determine the statistics of Fourier coefficients, but also those of the curvature $K(\varphi)=e''(\varphi)$ and of higher-order derivatives as well. Several results are known about the distribution of curvature in the case of stationary ensembles [13,15,25,26]. Here we shall point out some immediate conclusions that can be drawn from Fourier analysis concerning the statistics of an arbitrary level derivative $K_\alpha(\varphi)=e^{(\alpha)}(\varphi)$ (being analytic, levels have derivatives of all orders), under the scaling assumption (1.2).

From the very definition we get the mean square value of such a derivative in the form

$$\overline{K_\alpha^2} = \sum_{-\infty}^{+\infty} n^{2\alpha} |a_n|^2 , \qquad (2.18)$$

where, as usual, the bar denotes an average over the phase φ. On ensemble averaging this equation we get

$$\langle \overline{K_\alpha^2} \rangle = \Delta^2 \sum_{-\infty}^{+\infty} n^{2(\alpha-1)} c_n . \qquad (2.19)$$

From the scaling law we now obtain

$$\langle \overline{K_\alpha^2} \rangle \approx \Delta^2 \sum_{-\infty}^{+\infty} n^{2(\alpha-1)} \sqrt{c}\, P(n/\sqrt{c}) = A^{(2\alpha-2)} \Delta^2 c^\alpha , \qquad (2.20)$$

where $A^{(2\alpha-2)}$ is the $(2\alpha-2)$th moment of the distribution $P(t)$. From this equation, using the relation (2.5) between the moments of $P(t)$ and the derivatives of $C(\varphi)$ at $\varphi=0$, we obtain that the $(2\alpha-2)$th derivative of $C(\varphi)$ is singular at $\varphi=0$ if, and only if, the second moment of the αth derivative has nonintegrable singularities as a function of φ. On account of (2.17), this occurs when α is larger than 1,2,3, respectively, for GOE, GUE, GSE-like level repulsion. If, in addition, the PRM ensemble is stationary, then, for such values of α, the moments are divergent at all φ. For $\alpha=2$, that is, for ordinary curvature, and for $\beta\geq 2$, Eq. (2.20) establishes the propor-

tionality of rms curvature to the average kinetic energy,

$$\langle \overline{K_2^2} \rangle^{1/2} \approx \sqrt{A^{(2)}} \Delta c \approx \pi \sqrt{2b_2} \Delta c ,$$

where (2.5),(2.17) have been used to find $A^{(2)}$. This relation is similar to one found by Akkermans and Montambaux [27] for the case of symmetry-breaking AB flux, the difference being the additional φ average performed here. If, in addition, the ensemble is stationary, the same relation holds for the rms curvature at any point φ.

III. STATIONARY ENSEMBLES

A. Spectral correlations

The stationary ensembles we consider are defined by

$$H(\varphi)=H_1\cos\varphi+H_2\sin\varphi , \qquad (3.1)$$

where H_1,H_2 are fixed, (i.e., φ independent) random matrices, drawn independently from one canonical Gaussian ensemble (GOE, GUE, GSE). Depending on the chosen ensemble, the PRM ensemble defined by (3.1) has trajectories in different matrix spaces (the space of real symmetric matrices of rank N for GOE; of complex Hermitian matrices of rank N for GUE, of symplectic matrices of rank $2N$ for GSE). For every φ, the elements of the matrix $H(\varphi)$ are centered Gaussian random variables, of variance

$$\langle |(H_{1,2})_{ij}|^2 \rangle = \frac{1}{\beta N}(1+\delta_{ij}) . \qquad (3.2)$$

With the chosen normalization of matrix elements, the average eigenvalue density of $H(\varphi)$ obeys (in the $N\to\infty$ limit) the Wigner semicircle law [12] in the form

$$\rho(e)=\frac{N}{2\pi}(4-e^2)^{1/2} . \qquad (3.3)$$

In the central region of the spectrum the average level spacing is then $\Delta=\rho^{-1}(0)=\pi/N$.

Because Eq. (3.1) resembles the parametric equation of an ellipse, the PRM ensembles just defined will be termed "Gaussian elliptic" in the following. They have a number of distinguished features. In the first place, they are stationary [12,15]; therefore, all "pointwise" distributions, such as the distribution of velocity $e'(\varphi)$, of curvature $e''(\varphi)$, at given φ, are independent of φ. Moreover, two-point statistical correlations such as $\langle e'(\varphi_1)e'(\varphi_2) \rangle$ only depend on the difference $|\varphi_2-\varphi_1|$.

Second, at any φ the derivative $H'(\varphi)$ is statistically independent of $H(\varphi)$, and belongs to the same canonical ensemble; indeed, a simple computation shows that the matrix elements of both $H(\varphi)$ and of $H'(\varphi)$ are Gaussian distributed, and that they are uncorrelated. As a consequence, the level velocity $e'(\varphi)$ has a Gaussian distribution. In fact, $e'(\varphi)$ is given by an expectation value $\langle e|H'(\varphi)|e \rangle$ on the eigenvector $|e \rangle$ of $H(\varphi)$ corresponding to the eigenvalue $e(\varphi)$. On account of the independence of $H(\varphi)$ and $H'(\varphi)$, and of the rotational invariance of the Gaussian ensembles, such a matrix element must have the same distribution as any diagonal element

of $H'(\varphi)$. Therefore, it has a Gaussian distribution, with variance

$$\langle [e'(\varphi)]^2 \rangle = \frac{2}{\beta N} . \tag{3.4}$$

An independent (albeit more complicated) proof of the Gaussian distribution of level velocities can be obtained from supersymmetric calculations [7]. The variance (3.4) also follows from a statistical mechanical analysis of level dynamics (Eq. (3.8) of [15]) under the assumption of the applicability of the canonical ensemble.

Combining (3.4) with the mean spacing Δ we obtain for the center of the spectrum the average variance of level velocity (also called the average squared current)

$$c = \frac{2}{\beta \pi^2} N . \tag{3.5}$$

We have numerically computed Fourier transforms of eigenvalues $e(\varphi)$, for matrices of the above type, of rank $N = 40/400$. The eigenvalues were unfolded in order to normalize them to unit level spacing. In computing (fast) Fourier transforms we have used grids of $128/1024$ points in $(0, 2\pi)$—the optimal size of a grid grows with the matrix rank N. To avoid confusion, in the following the results of averages over φ taken for a fixed level and a fixed realization will be called "mean values," while by "average values" we shall mean results of statistical averaging (over realizations, and/or over different levels). Thus mean values will be fluctuating quantities, in contrast to average values. For each level we have computed Fourier coefficients a_n, mean correlation Fourier coefficients r_n [defined by Eq. (2.11)], and the mean squared velocity $r = \sum r_n$. Finally, statistical averages were taken over all the eigenvalues lying in the central half of the spectrum, and the results were further averaged over samples of $20/300$ matrices.

As a first step, we have checked the scaling law (1.2). The numerically computed moment $\langle |n| \rangle$, defined by (2.4), grows as $\sqrt{N}$, hence, as $\sqrt{c}$, as predicted by the scaling law. Moreover, the relative width of the Fourier spectrum, measured by $\delta_n := (\langle n^2 \rangle - \langle |n| \rangle^2)^{1/2} / \langle |n| \rangle$ is constant, as required. Direct evidence for the scaling law in the GUE case is presented in Fig. 2, where the function $P_2(t)$ is plotted for various matrix sizes N against the rescaled variable $t = n / \langle |n| \rangle$.

All the assumptions that underlie the argument developed in the preceding section appear to be satisfied for elliptic ensembles, so that the small-φ behavior (2.17) or, equivalently, the large-t behavior (2.16) are expected.

Some of the coefficients b, which belong to the nonsingular part of the expansion (2.17), are explicitly known,

$$b_2 = 2, \quad b_4 = \tfrac{8}{3} \tag{3.6}$$

as can be obtained [16] by expanding $C(\varphi)$ around $\varphi = 0$ to the lowest nonvanishing order, and using for the variance of curvatures, $\langle [e''(\varphi)]^2 \rangle$, the values derived from
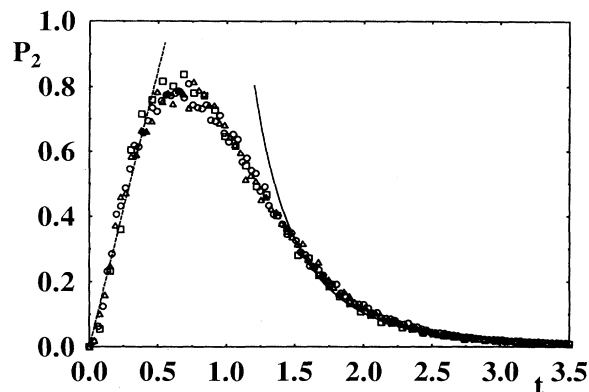

FIG. 2. Illustrating the scaling law (1.2) in the Fourier domain for the elliptic GUE. The universal function $P_2(t)$ [Eq. (2.14)] versus $t = n / \langle |n| \rangle$ for matrices of rank $N = 71(\square)$, $N = 300$ ($\triangle$), $N = 400$ ($\circ$). Lines show the initially linear rise and the t^{-4} tail.

exact curvature distributions [15,25,26]. The coefficient b_2 has also been found via supersymmetric calculations [7]. In the case of rank-2 matrices we have exactly and explicitly calculated the functions C_1, C_2, which are reported in the Appendix and have the predicted small-φ behavior.

In numerically analyzing the large-n behavior of the coefficients c_n, two competing numerical effects, which obscure the real asymptotics, have to be taken into account. The first is "aliasing," an artifact originated by the discretization used in Fourier transforms, which tends to bend the numerical tails upward. A second effect, which tends to bend them downward, is due to finite statistics: however large the sample of matrices, the avoided crossings sampled in it have a finite nonzero minimum width, that will be detected by the Fourier transform as soon as n becomes large enough. To get rid of such effects, we have just restricted our attention to that part of the c_n sequence that proved stable against in-
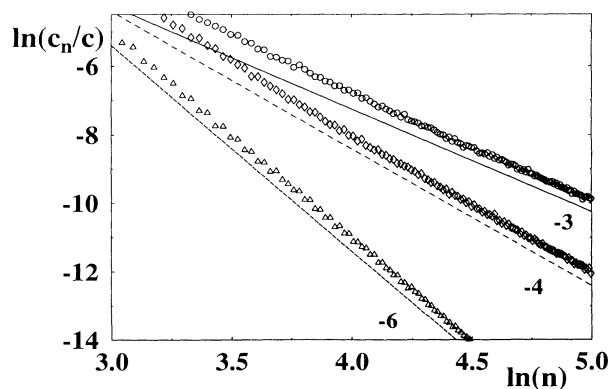

FIG. 3. Large-n decay of the Fourier coefficients of the correlation function, for the three elliptic ensembles: GOE ($\circ$), GUE ($\Diamond$), GSE ($\triangle$). Lines (with slopes indicated in the figure) correspond to algebraic tail behavior.
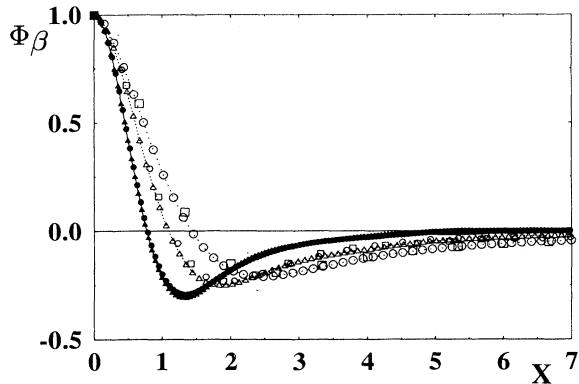
FIG. 4. Scaling functions $\Phi_\beta(X)$ versus the rescaled parameter X for elliptic ensembles and different matrix rank N: GSE (filled symbols) with $N=80$ (triangles) and $N=90$ (circles); GUE (open small symbols) with $N=71$ (triangles), $N=300$ (circles), and $N=400$ (squares); GOE (large symbols) for $N=80$ (circles) and $N=400$ (squares).

creasing the Fourier transform basis and the size of the sample. Results are shown in Fig. 3 for the three cases $\beta=1,2,4$, and agree with the prediction $c_n \sim n^{-2-\beta}$.

Finally, we have used the numerical Fourier transforms to reconstruct the scaling functions $\Phi_\beta(X)$. Results are shown in Fig. 4 for the three elliptic ensembles, and in more detail in Fig. 5 for GUE. In this case, we have compared the empirical Φ_2 with the theoretical predictions, Eqs. (2.17) at small X, and X^{-2} at large X, finding a good agreement in both cases.

B. Statistics of Fourier coefficients

An arbitrary rotation $\varphi \mapsto \varphi+\alpha$ results in multiplication of the Fourier coefficients a_n by the phase factor $e^{in\alpha}$. On the other hand, such a rotation must leave the statistics of the stationary ensemble unchanged. Hence $\langle a_n \rangle = e^{in\alpha}\langle a_n \rangle$, and, since α is arbitrary, $\langle a_n \rangle = 0$. A quite similar argument shows that $\langle a_n^* a_m \rangle = 0$ if $n \neq m$, which means that the complex variables a_n are pairwise uncorrelated. Nevertheless, they cannot be statistically independent. In fact, for any fixed realization they decay exponentially fast at large n, but their variances decrease algebraically instead. This sharp contrast between the individual and the average decay entails a strong statistical dependence between coefficients a_n at large n.

Formula (2.6) shows that a_n are sums of a large number $\sim \sqrt{c} \sim \sqrt{N}$ of contributions I_j, that come from the different BP's. On assuming these contributions to be independent, one would naturally expect a Gaussian distribution for a_n, which implies an exponential distribution (χ_2^2) for $|a_n|^2$. Numerical computations have confirmed this prediction for all three universality classes and $n=1,2,3$ with $N=50$. However, at very large n the asymptotics (2.6),(2.9) hold, with only a few terms surviving in the sum, corresponding to very small, and unlikely, avoided crossings. In this case, a Gaussian distribution can hardly be expected. A Gaussian distribution of *all* the Fourier coefficients can be, in fact, ruled out: for otherwise, these coefficients, being uncorrelated, would also be independent, a case that we have just excluded. In addition, other variables linearly depending on the a_n such as, e.g., the curvature $K(\varphi) = -\sum_n n^2 a_n e^{in\varphi}$ should have a Gaussian distribution [34], which is known to be false [15,25,26].

Our numerical data have revealed broad, non-Gaussian tails of the distributions of the real and the imaginary parts of a_n for sufficiently large n. In Fig. 6, we illustrate the transition from a Gaussian to a non-Gaussian distribution of a_n, which occurs as n increases, by plotting the logarithmic variance [i.e., the variance of $\ln(|a_n^2|)$] versus $t = n/\langle |n| \rangle$, for the case of elliptic GUE. The logarithmic variance corresponding to a Gaussian distribution of
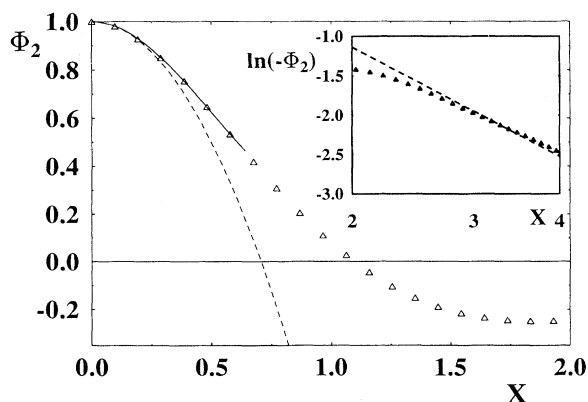

FIG. 5. The Scaling function $\Phi_2(X)$ for the elliptic GUE, matrix rank 71. The dashed line is the second-order expansion $1-2X^2$; the solid line includes a third-order term $+1.033X^3$. The inset illustrates the X^{-2} behavior at large X.
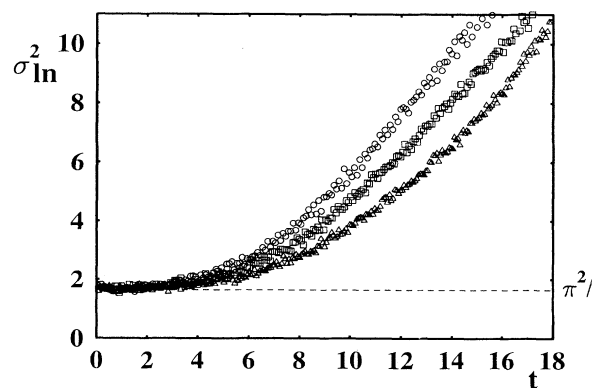

FIG. 6. Variance $\sigma_{\ln}^2$ of $\ln(|a_n|^2)$ versus of $t=n/\langle n \rangle$ for the elliptic GUE and $N=40$ ($\circ$), 60 ($\square$) and 80 ($\triangle$). The horizontal dashed line corresponds to (complex) Gaussian distribution of a_n.

a_n is equal to $\pi^2/6$; this value is indeed found at small $n < \langle |n| \rangle$ (for $N = 40, \langle |n| \rangle \approx 12$), but not at larger n, yielding evidence that the distribution of Fourier coefficients is not Gaussian anymore. Moreover, the same Fig. 6 shows that the logarithmic variance does not scale with $n/\langle |n| \rangle$. Therefore, although the second moments of the Fourier coefficients scale in a simple way (1.2), uniformly (that is, for all n), the same is not true for their global statistical distribution, except perhaps in the range $n < \sqrt{c}$, where, due to the Gaussian character of the distribution, the scaling of the second moments entails the scaling of all moments.

C. Curvatures and mean kinetic energy

Equation (2.20), and its consequences, are obviously valid in the case of Gaussian elliptic ensembles. In addition, $\langle \overline{K_\alpha^2} \rangle = \langle K_\alpha^2(\varphi) \rangle$ for all φ because of the stationarity of the ensemble. From Eqs. (2.17), (2.5), and (3.6) one finds $A_2^{(2)} = 4\pi^2$ and $A_4^{(2)} = 16\pi^2/3$. Thus, in particular, in the elliptic GUE the rms of the curvature is, at any point φ, proportional to c, with a factor $2\pi\Delta$.

The Gaussian distribution of the level velocities entails a Porter-Thomas distribution of squared velocities. Nevertheless, such a distribution cannot be expected for the mean-square level velocity $r = \sum_n r_n$ [the square level velocity, averaged over φ; a realization-dependent quantity, see Eq. (2.10)], which is *not* the square of a Gaussian variable. Braun and Montambaux [10] have numerically studied the distribution of r for the three-dimensional (3D) Anderson model in the metallic regime, and have approximated their data by a logarithmic-normal distribution. In this section, we describe our results for the distribution of r in the elliptic GUE.

Our data show that the variance σ_r^2 of r is proportional to $N^{3/2}$, while the logarithmic variance $\sigma_{r\ln}^2 = \langle \ln^2(r) \rangle - \langle \ln(r) \rangle^2$ scales as $N^{-1/2}$. Thus the relative fluctuation of r vanishes in the limit $c \to \infty$, that is, r/c is a self-averaging quantity. Figure 7 displays the
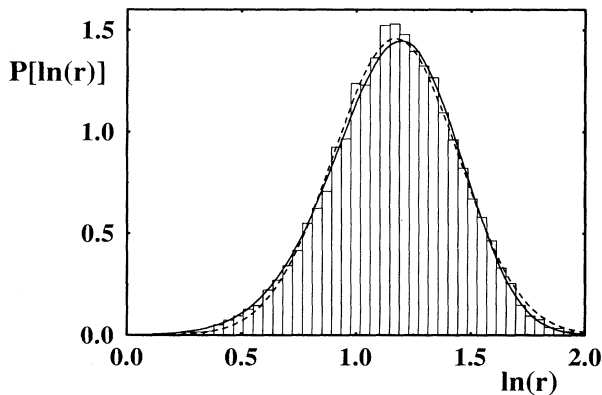

FIG. 7. Distribution $P(\ln r)$ of the logarithm of the mean-square current, for the elliptic GUE obtained from 200 realizations of rank $N = 40$. The dashed line represents the logarithmic-normal distribution with $\langle \ln(r) \rangle = 1.17$ and $\sigma_{\ln}^2 = 0.075$; the solid line corresponds to the χ_ν^2 distribution, with mean $c = 3.34$ and number of degrees of freedom $\nu \approx 2/\sigma_{\ln}^2$.

distribution $P(\ln(r))$ of the logarithm of r obtained from 200 GUE matrices with $N = 50$. The small but significant asymmetry with respect to the mean advises against a Gaussian fit; as a matter of fact, a much better fit for the empirical distribution of r was obtained by means of a $\chi_\nu^2(r)$ distribution, with the average $\langle r \rangle = c$, and with the number of degrees of freedoms $\nu \approx 2/\sigma_{r\ln}^2$. The latter estimate follows from the observation that the logarithmic variance $\sigma_{\ln}^2$ of the χ_ν^2 distribution does not depend on the mean and is given by $\Psi'(\nu/2)$ where the trigamma function [29] $\Psi'(\nu/2) \sim 2/\nu$ at large ν. The resulting distribution (solid line in the figure) fits the data much better than the log-normal distribution. A similar distribution describes the mean kinetic energy statistics for GOE and GSE.

As already mentioned, $\sigma_{r\ln}^2$ depends on the matrix size as $N^{-1/2}$. Hence ν is proportional to $\sqrt{N}$ and also to the mean coefficient $\langle n \rangle$; in other words, the number of degrees of freedom is proportional to the width of the Fourier spectrum. Numerical data give for GUE $\nu \approx 3\langle |n| \rangle$. Therefore, our results appear to indicate that the statistics of $r = \sum_n n^2 |a_n|^2$ are determined only by the Fourier amplitudes a_n with $n < \sqrt{c}$, which, as we know, are Gaussian and uncorrelated. This would also explain the observed dependence of the variance of r, for

$$\sigma_r^2 \sim \sum_{|n| < \sqrt{c}} c_n^2 \sim c^{3/2} \int_0^1 P^2(t) dt \ . \tag{3.7}$$

This interpretation is far from complete, though. In fact the scaling law implies that the relative contribution to r of the region $n > \sqrt{c}$ is independent of c, so that there is no *a priori* reason why it should be negligible.

IV. PERIODIC BAND RANDOM MATRICES

A. General properties

Let us consider a circular array of N sites on a ring, labeled by the index $j = 1, \ldots, N$. By definition, a PBRM has nonzero matrix elements $H_{jk}(\varphi)$ only for sites which are no more than b sites apart *on the circle*, where $b \leq N$ is an integer specifying the width of the band. The matrix elements are further specified by

$$H_{jk}(\varphi) = \begin{cases} h_{jk} & \text{if } |j - k| \leq b \\ h_{jk} e^{i\varphi} & \text{if } j \leq k + b - N \\ h_{jk} e^{-i\varphi} & \text{if } j \geq k + N - b \ , \end{cases}$$

where h_{jk} are real Gaussian variables, independent of φ, $h_{jk} = h_{kj}$, with the normalization

$$\langle h_{jk}^2 \rangle = \frac{N+1}{2bN} (1 + \delta_{jk}) \ . \tag{4.1}$$

For an odd value of N and $b = (N+1)/2$ we get at $\varphi = 0$ a full GOE matrix.

PBRM's are obtained from a Bloch decomposition of infinite, periodic, banded random matrices, and φ is the corresponding Bloch index. The PBRM ensemble differs from the periodic random matrix ensembles matrices considered above in the following two important respects:

(1) $H(\varphi)$ exhibits a proper diffusive regime in the range $1 \ll b \ll N \ll b^2$ (which should not be identified with the ballistic regime $b \approx N$), and a localized regime at $N > b^2$. All statistical properties of $H(\varphi)$ depend on b and N through the scaling variable $x = b^2/N$, which is proportional to the ratio between the localization length of the eigenfunctions in the limit $N = \infty$ and the "sample size" N [8];

(2) The self-adjoint matrix $H(\varphi)$ satisfies $H(-\varphi) = H^*(\varphi)$. Therefore, at $\varphi = 0$ and $\varphi = \pi$ the matrix $H(\varphi)$ is real symmetric, while at any other value of φ it is complex Hermitian. This is exactly the behavior expected for a Hamiltonian depending on an Aharonov-Bohm magnetic flux.

On account of both the properties mentioned above, PBRM's provide a model for the dynamics of electrons in small disordered rings threaded by a magnetic flux φ (in dimensionless units). Previous studies [8] have shown that the behavior of the ensemble-averaged, zero-flux scaled absolute curvature $\mathcal{H} := \Delta^{-1} \langle |e''(0)| \rangle$ is quite similar to the one expected of the average conductance in the scaling theory of localization. The distribution of $\mathcal{H}$ also depends on x, being identical to the generalized Cauchy distribution (first conjectured by Zakrzewski and Delande [15], and then proven for the GUE [25] and for a broad class of ensembles of random matrices [26]) in the delocalized limit $x \to \infty$, and resembling a logarithmic-normal distribution in the opposite localized limit. In general, all statistical properties change continuously as the delocalization parameter varies from the localized to the delocalized limit. For instance, Fig. 8 shows the x dependence of the averaged squared current c, the variance σ_r^2, the logarithmic-variance $\sigma_{r\,\ln}^2$, and the moment $\langle |n| \rangle$ of the Fourier spectrum. The latter is close to unity in the localized regime; but in the diffusive regime it scales as $\sim x^{1/2}$. This result has a simple explanation: the Thouless conductance $\langle |K(0)| \rangle \Delta^{-1}$ obeys Ohm's law in the diffusive regime [8], hence it is proportional to x. On the other hand, according to a relation discussed by Akkermans and Montambaux [27] and numerically verified for the PBRM [8] and the 3D Anderson model [9], in that regime the Thouless conductance is also proportional to $C_{AB}(0)$. Therefore, $c \sim x$, and $\langle n \rangle \sim \sqrt{c} \sim \sqrt{x}$. For the same reason, on approaching the extreme delocalized regime some power-law dependences on $c \sim x$ are recovered, which are typical to canonical ensembles of "full" random periodic matrices: e.g., $\sigma_r^2 \sim x^{3/2}$, $\sigma_{r\,\ln}^2 \sim x^{-1/2}$ and $\delta_n = \text{const}$.

Though the general approach described in Sec. II is still valid, some modifications of the picture described for the elliptic ensembles are imposed by the specific features of the PBRM ensemble; in the first place, by the symmetry breaking occurring at $\varphi = 0$, due to which this ensemble is not stationary. One-point spectral statistics (level spacing distributions, curvature distributions, ...) change as φ is increased from 0 to some value φ_c which is however small, in the sense that it decreases with $1/\sqrt{c}$; at large c the transition is, therefore, a very sharp one [30]. The correlation analysis of Sec. II cannot be literally replicated for the PBRM model, as the distribution of BP's in the complex φ plane cannot be homogeneous in
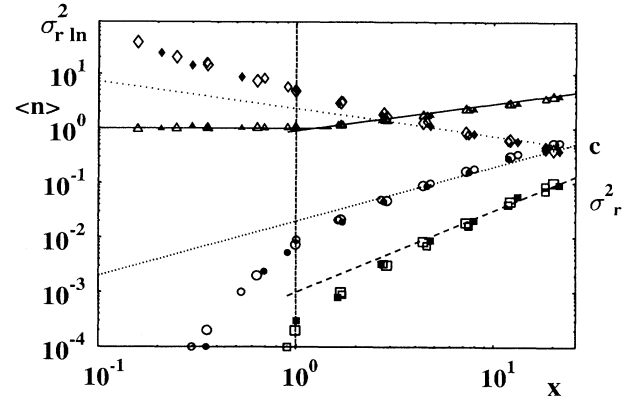

FIG. 8. Illustrating the power-law dependence of various ensemble averages on the scaling parameter $x = b^2/N$, for periodic banded random matrices of rank 71 (small open symbols), 101 (small filled symbols), 201 (large open symbols). Average squared current $c = \langle r \rangle$ ($\circ$), mean current variance σ_r^2 ($\square$), logarithmic-variance $\sigma_{r\,\ln}^2$ ($\diamond$), width of the Fourier spectrum $\langle |n| \rangle$ ($\triangle$). Lines represent the limit dependences that are approached in the delocalized regime. The vertical line is somewhat arbitrarily drawn to represent the transition from localization to delocalization.

φ; the width γ of a complex branch point may not be statistically independent on its location φ_0, because of the changes of symmetry occurring at special values of φ. We have, therefore, to investigate how the statistical distribution of BP's is affected by the symmetry breaking. This is, in turn, closely related to the distribution of avoided crossing sizes (gaps) and their positions, which will be analyzed below.

B. Avoided crossings

The above mentioned symmetry of the PBRM model entails that eigenvalues $e(\varphi)$ are symmetric with respect to $\varphi = 0$ ($\varphi = \pi$), and their velocities vanish there. It follows that relative extrema for the level spacings are observed at these symmetry-breaking values of φ. In other words, a large set of avoided crossings (relative *minima* of spacings) must appear at a *fixed* value of $\varphi = 0$ (or π). Thus, with probability one, there will be BP's lying on the lines $\varphi = 0, \pi$. Such BP's will contribute a δ-function term in the distribution of real parts φ_0 of BP's. Moreover, since the width of any of these avoided crossings is at once a nearest-level spacing, the distribution of these widths, at small values, will behave exactly like the level spacing distribution at $\varphi = 0, \pi$, hence with the exponent $\beta = 1$ (and not $\beta - 1$, as with BP's having a random position).

We, therefore, infer that the symmetry-breaking lines contribute a singular term to the distribution $p(\gamma, \varphi)$ of BP's in the complex plane, of the form (apart from a normalization constant):

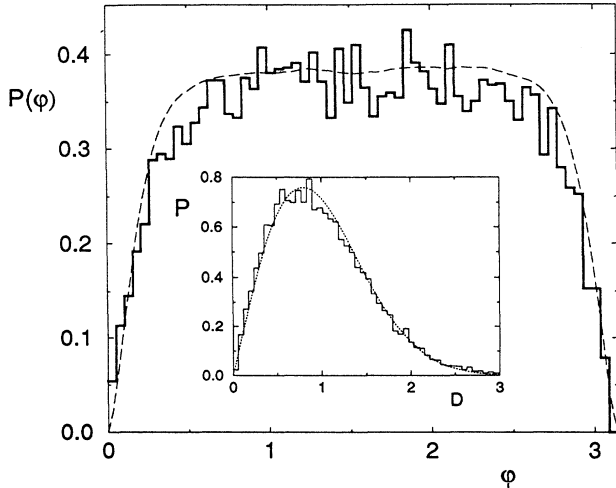$$p_s(\gamma, \varphi) = [\delta(\varphi) + \delta(\varphi - \pi)] f_0(\gamma) \tag{4.2}$$

FIG. 9. Abundance of avoided crossings as a function of φ for the PBRM ensemble (150 matrices with $N = 201, b = 64$). The histogram has been obtained from 4452 avoided crossings occurring inside the open $(0,\pi)$ interval, in which only eigenvalues belonging in the central half of the spectrum were involved. The dashed line is proportional to the average squared level velocity. The inset compares the distribution of avoided crossing sizes (normalized to a unit mean gap) with the Wigner distribution.

with $f_0(\gamma) \sim \gamma$ at small γ. We shall now examine the other type of avoided crossings, namely those which have fluctuating positions *inside* the $(0,\pi)$ interval. In order to numerically compute the positions and sizes of avoided crossings we have used the same procedure as in previous studies on stationary ensembles; we refer the interested reader to [24] for details.

In Fig. 9, we illustrate the distribution of the positions of the "fluctuating" avoided crossings lying inside $(0,\pi)$, for matrices belonging to the diffusive regime. A strong dependence of the abundance of avoided crossings with respect to φ is apparent. In particular, fluctuating BP's appear to be repelled by the symmetry-breaking values (where, as remarked above, other BP's already exist). The abundance of fluctuating avoided crossings depends on the position φ in a way that resembles that of the average squared level velocity, which will be discussed later.

Although the distribution of avoided crossings is not homogeneous in φ, the (conditional) distribution of their sizes appears to be the same at all $\varphi \neq 0, \pi$ and is presented as an insert in Fig. 9. Thus we argue that the BP's located inside $(0,\pi)$ contribute a "smooth" part $p_0(\gamma, \varphi)$ to the total density of BP's, which is not φ independent in the vicinity of $0,\pi$, but is $\sim \gamma$ at small γ, at all φ.

C. Spectral correlations

On the grounds of the above discussion, the distribution of the BP's in the complex plane consists of a "smooth" part, given by the BP's internal to $(0,\pi)$, plus a "singular" part, exactly located on the symmetry break-

ing lines. *In both parts, the probability of small γ scales with the same exponent* 1. The correlation analysis of Sec. II now applies unaltered to the effect that the type of singularity exhibited by $C_{AB}(\varphi)$ at $\varphi = 0$ is of GUE type, like that of $C_2(\varphi)$; the numerical coefficients, nevertheless, may be different (and will indeed become different on moving towards the localized regime).

On numerically computing Fourier transforms, we have, in fact, found distributions c_n whose general features cannot be distinguished from those observed in the pure GUE case, on the level of accuracy of our computations. In particular, a decay $c_n \sim n^{-4}$ is apparent (Figs. 10 and 11). The corresponding correlation functions are almost identical to those obtained for the elliptic GUE case (Fig. 12).

The n^{-4} decay is by no means consistent with the behavior suggested by Braun and Montambaux [10], which is instead of the type exhibited by $C_1(\varphi)$ in (2.17) and would, therefore, result in a n^{-3} decay. Berry and Keating (BK) [17] have proposed an explicit semiclassical approximation for C_{AB}, which is compared with the numerically computed CF for the PBRM model in Fig. 10. A free parameter w^*, which appears in the BK formula, has been fixed by means of a one-parameter fit to our data for $N = 201, b = 64$. The obtained value $w^* = 3.92$ is quite small; therefore, we have used Eq. (28) of Ref. [17], instead of its limiting form, Eq. (29), which is valid in the limit of large w^*. Including the "nondiagonal" correction [17] yields no significant improvement to the fit. The minimum of the semiclassical CF is too shallow as compared to numerical data (see inset in Fig. 10). Moreover, since the C_{AB} of BK is an analytic function at all real φ, its Fourier transform has an exponentially decaying tail,
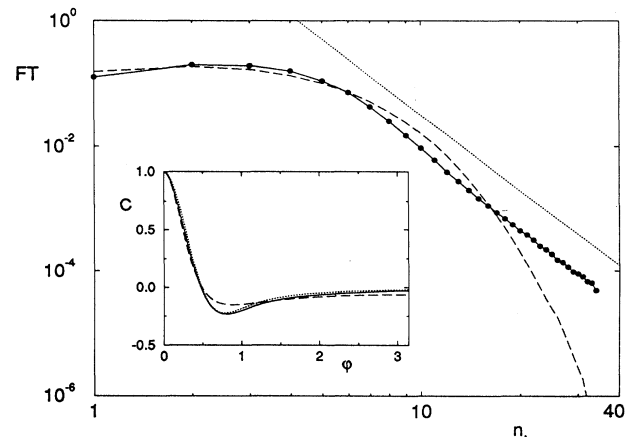

FIG. 10. CF for the PBRM ensemble in the diffusive regime ($N = 201, b = 64$ (inset, full line) and its Fourier transform (main panel, filled circles). The dotted line represents the n^{-4} decay. Both in the main figure and in the inset, dashed lines represent the Berry-Keating semiclassical approximation. The dotted line in the inset represents a semiempirical formula proposed in Ref. [16].

at variance with the real algebraic tail (main panel in Fig. 10) [35].

It is worth pointing out, as a purely empirical observation, that a significant *de facto* agreement with numerical data is provided by a recently proposed semiempirical representation of the CF [16], which we show in the same inset. No fitting was used in this case, the only adjustment being the rescaling from the dimensionless parameter X (for which the semiempirical representation of CF was given) to φ. Different data sets (e.g., for $N=201, b=101$, close to the ballistic regime, with $w^* \approx 6.35$) have shown an even better agreement with this analytical representation (while no significant improvement has been observed with the BK formula).

Nevertheless this semiempirical representation, too, is in the form of an analytic function, and cannot, therefore, correctly represent the small-φ behavior. Like the BK formula, in the Fourier domain it yields exponential instead of algebraic tails, at variance with numerical data.

On moving towards the localized regime, the $C(\varphi)$ curve undergoes a continuous deformation (Fig. 12), and the singularity at $\varphi=0$ remains of the same type all the way down to the deeply localized regime; in fact, Fourier transforms always exhibit a $|n|^{-4}$ tail. In all the investigated range we have obtained evidence that $C(\varphi)$ depends on b,N only through the localization ratio $x=b^2/N$: $C(\varphi,b,N)\approx C(\varphi,x)$ at $b,N\gg 1$. In the diffusive regime, $x>1$, the scaling (1.2) is still approximately valid: $C(\varphi,x)\approx c(x)\Phi_{AB}[\pi\varphi\sqrt{c(x)}]$ with $c(x)=C(0,x)\sim x$ (weak-localization corrections are hardly assessed at the present level of accuracy). As an illustration, we plot in Fig. 13 the position $\varphi_0(x)$ of the zero of $C(\varphi,x)$, as a function of x. In the diffusive part of the plot, $\varphi_0(x)$ is proportional to $1/\sqrt{x}$, consistently with (1.2) and with $c\sim x$. In the localized regime this scaling is not valid any more. The Fourier spectrum shrinks exponentially fast; all the harmonics except the first tend to disappear, so that $C(\varphi)$ tends to $c\cos\varphi$.
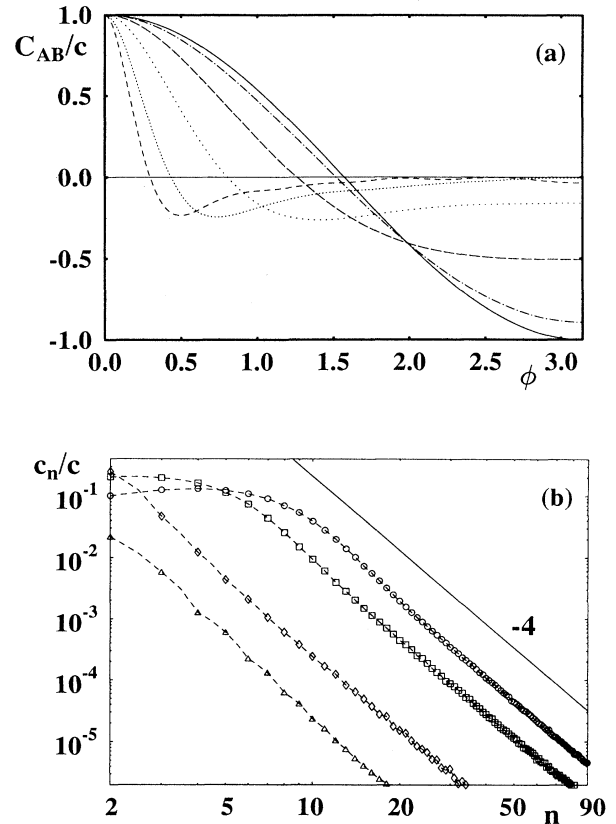

FIG. 12. Correlation function for the PBRM ensemble (a), and its Fourier transform (b), for various values of the localization parameter x. Numerical data in (b) are for matrices of rank $N=201$ and $b=101,64,23,9$ from rightmost to leftmost curve. All the reported data sets have the same slope, even in the localized regime (for $b=9,\ln(x=b^2/N)\approx -1$).
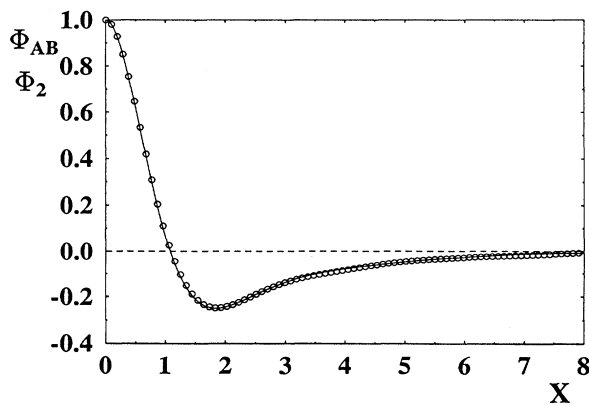

FIG. 11. Comparison of the scaled correlation functions Φ_2 for the elliptic GUE with $N=71$ (circles) and Φ_{AB} for the PBRM ensemble with $N=101, b=51$ (shown by a continuous line, obtained by interpolating numerical data).
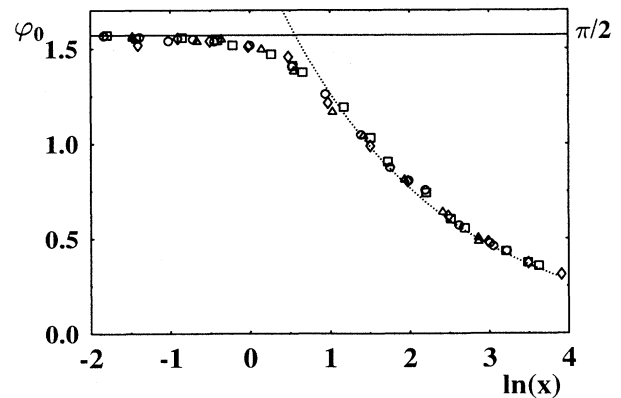

FIG. 13. The position φ_0 of the zero of the CF for the PBRM ensemble, versus the localization parameter $x=b^2/N$ for matrices of rank 200,150,100,70. The dotted curve corresponds to $\varphi_0=6.55/x^{1/2}\pi$.

D. Statistics of Fourier coefficients

In the PBRM ensemble, the Fourier coefficients a_n are real. Our numerical data for their statistical distributions show in the delocalized regime a behavior similar to the one observed for stationary ensembles. At small $n < \langle n \rangle$ we obtained a Gaussian distribution of a_n; as a consequence, the logarithmic variance $\sigma_{\rm in}^2$ [i.e., the variance of $\ln (a_n^2)$] is constant and equal to $\pi^2/2$. For n larger than $\langle n \rangle$ the distribution exhibits broad, exponential tails (Fig. 14).

On the other hand, in the localized regime, none of the coefficients is Gaussian distributed.

In the stationary case, the assumption that the phases φ_{0j} of the BP's come at random immediately leads to the vanishing of correlations between different a_n—a result that we have obtained in a different way, and which is intimately linked to the stationarity of the ensemble. In the PBRM case, which is not stationary, different Fourier coefficients have nonzero correlations; the asymptotic formula (2.9) can be used together with formula (2.6) to study the correlation matrix $\langle a_n a_m \rangle$.

The random phase assumption is not legitimate for the BP's that have nonrandom phases $0, \pi$. From (2.6),(2.9) it follows that these BP's contribute a correlation

$$\langle a_n a_m \rangle \sim [1+(-1)^{n+m}]\left\langle \gamma \frac{e^{-\gamma(|n|+|m|)}}{|nm|^{3/2}} \right\rangle$$

$$\sim [1+(-1)^{n+m}]M\frac{1}{|nm|^{3/2}(|n|+|m|)^3}$$

$$(4.3)$$

with M a numerical factor. In estimating the ensemble average, the GOE-like distribution of small γ of BP's lying on the symmetry lines was used. We shall neglect the contributions of the remaining BP's, which have fluctuating phases. The formula (4.3) will be used in the next sec-
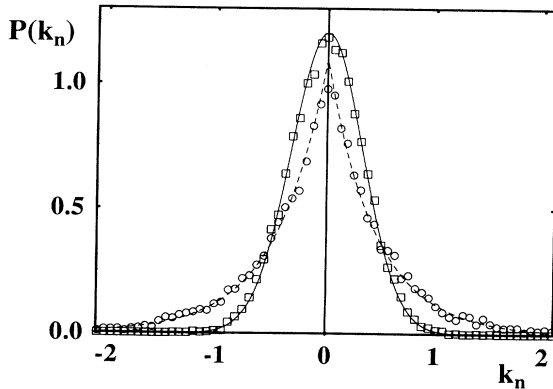
tion to analyze the behavior of certain quantities near the symmetry-breaking point $\varphi=0$.

E. Kinetic energies and curvatures

From the expansion

$$\langle e'^2(\varphi) \rangle = \sum_n \sum_m nm \langle a_n a_m \rangle e^{i(n-m)\varphi} ,$$

we obtain, using (4.3),

$$\langle e'^2(\varphi) \rangle = \sum_k B_k e^{2ik\varphi} ,$$

where the coefficients B_k have the asymptotic behavior

$$B_k \sim M \sum_p \frac{|k^2-p^2|^{-1/2}}{\max(|k|,|p|)^3} \sim \frac{1}{|k|^3} .$$

As we know, such an asymptotic behavior of the Fourier expansion entails a singularity at $\varphi=0$, of type $\langle e'^2(\varphi) \rangle \sim \varphi^2 \ln|\varphi|$ (and a similar behavior close to $\varphi=\pi$), as predicted in [31] for a GOE-GUE transition and numerically observed for the Anderson model [10,30].

A quite similar analysis shows that the second moment of the curvature has a logarithmic singularity at $\varphi=0,\pi$, as again it was predicted in [31,10] [36].

Figure 15 shows the dependence of the average squared velocity (normalized to its maximal value) as a function of the scaling variable, $X = \pi\varphi\sqrt{c}$, for $N=71$ and for several band widths b. Our numerical data are consistent with the mentioned logarithmic behavior. Moreover, in the delocalized regime, the data for different values of b follow the universal dependence recently predicted for the GOE-GUE transition [32]

FIG. 14. Distribution of the coefficient $k_n = n^2 a_n$ for the PBRM ensemble, with $N=61, b=31$, and for $n=1$ (Gaussian) ($\square$), and $n=10$ [non-Gaussian, with exponential tails, $\exp(-k_n)$] ($\bullet$).
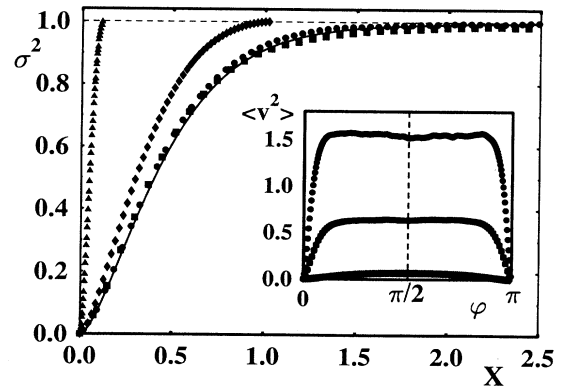

FIG. 15. Average squared velocity $\sigma^2 = \langle [e'(\varphi)]^2 \rangle$ (normalized to its maximum value) versus the rescaled phase X, for the PBRM ensemble with $N=201$ and $b=9$ ($\triangle$), 23 ($\Diamond$), 64 ($\square$), and 101 ($\bullet$). In the delocalized regime numerical data agree with the theoretical formula for Taniguchi et al. [32] (solid line). The insert shows the same data without rescaling.

$$\frac{\langle [e'(\varphi)]^2 \rangle}{e'^2_{max}} = 1 - \frac{\sqrt{\pi/2}\, \mathrm{erfi}(\sqrt{2}X)[1+2X^2\exp(2X^2)\mathrm{Ei}(-2X^2)]}{2X\exp(2X^2)} , \qquad (4.4)$$

where Ei( ) denotes the exponential integral and $\mathrm{erfi}(x) = -i\,\mathrm{erf}(ix)$ is the imaginary error function [29].

The statistics of the mean kinetic energy is similar to the one discussed for elliptic ensembles; again, the distribution $P(r)$ is better approximated by a χ^2_ν distribution than by a logarithmic-normal one. In the localized regime, the width of the distribution $P[\ln(r)]$ increases with decreasing x. As shown in Fig. 8, on decreasing x the logarithmic variance $\sigma^2_{r\ln}$ grows faster than $x^{-1/2}$.

The relation (2.20) is still valid, as is the proportionality between the width of the curvature distribution $P(K)$ at $\varphi = 0$, measured by $g_1 = \langle |K(0)| \rangle$, and c [27,8]. The proportionality constant is close to 2π, as numerically observed for the Anderson model [10] and analytically found in [26]. Localization effects produce deviations from both proportionality relations at $x \ll 1$ [9,8].

Within the above described Fourier framework, it is also possible to analyze how the distribution of the curvature $K(\varphi)$ depends on φ. This problem is also attracting interest; here we shall just make some qualitative remarks, deferring a more detailed analysis to future publications. The curvature distribution is affected by the distribution of BP's in the vicinity of the chosen point φ on the real axis; in fact BP's coming very close to this point determine large curvatures, hence their statistical distribution determines the tail of the curvature distribution. However, the singular and the smooth parts of the BP distribution contribute in a different way in this tail. The singular part yields a relatively large probability for BP's coming close to $\varphi = 0, \pi$, which in turn yields a large probability of large curvatures there; as a matter of fact, the curvature distribution at $\varphi = 0, \pi$ was found to be of the Zakrzewski-Delande type [8]. Nevertheless, the same BP's, being bound to the lines $\varphi = 0, \pi$, cannot come arbitrarily close to a point $\varphi \neq 0, \pi$, and cannot, therefore, produce large curvatures there. In fact, if *only* the singular part of the BP distribution is taken into account, then a simple estimate based on (2.6), (2.9), and (4.3) shows that at $\varphi \neq 0, \pi$ all the moments of $K(\varphi)$ are finite. Therefore, in any ensemble for which a smooth part is missing, the tail of the curvature distribution at $\varphi \neq 0, \pi$ decreases faster than any power of curvature. This is exactly the case with the 2×2 matrix ensemble considered in [31], where all BP's lie at $\varphi = 0$ ($\gamma = 0$ in the notation of [31]), and the curvature distribution was in fact shown to have Gaussian tails at $\varphi \neq 0$.

Short of being typical of ensembles exhibiting a magnetic flux-induced GOE-GUE transition, such a behavior rather appears as an artifact of ensembles lacking the smooth part of the BP distribution; the presence of such a part would in fact restore a chance for BP's coming close to *any* point on the real line. The impact of this fact on the curvature distribution is currently under investigation.

V. CONCLUSIONS

In this paper, we have illustrated the usefulness of analytic continuation to complex parameter values in the analysis of various statistics of parametric level dynamics, which are essentially determined by the statistical distribution of complex level crossings, i.e., of the singularities of branch-point type exhibited by the eigenvalues as functions of the complex parameter. Though this approach is not, for the time being, as powerful as other methods (such as, e.g., supersymmetric ones), it offers, in or opinion, a particularly perspicuous picture.

Our analysis was, in many respects, a heuristic one, although one rigorous result was also given: independently of symmetry, the level velocity correlation function can be analytic only if the matrix ensemble is so built as to make too narrow avoided crossings impossible. Thus in most cases this correlation function has singularities, which have the same origin as the divergence of the second moments of certain level derivatives, to which they are, in fact, connected by the relation (2.20). The latter is in a (rather superficial) sense a generalization of the Akkermans-Montambaux relation for conductance.

Our estimates for the singularities of the correlation function were confirmed by numerical simulations, and also cover the physically important case, in which the parameter has the meaning of an Aharonov-Bohm flux. This case was modeled by the PBRM ensemble. Unlike most of the usually considered ensembles, which consist of "full" random matrices, this ensemble exhibits a proper diffusive regime in a suitable parameter range, marked by an ohmic dependence of the average curvature on the matrix size; therefore, the corresponding eigenfunctions, although delocalized, have to differ from those of "full" random matrices in some as yet not fully understood, but nonetheless essential respect. The investigation of this ensemble has confirmed that various scaling properties, originally established for conventional ensembles, remain substantially valid in the diffusive regime (already investigated in [10] for a different model).

The GOE-GUE breaking of symmetry that occurs on switching on the Aharonov-Bohm flux appears to have no impact on the behavior of the correlation function, which looks the same as for a homogeneous GUE. Nevertheless, the transition is reflected by a singular behavior of other quantities. Some features of this transition, such as, e.g., the way it affects the curvature distribution, are not yet understood, as they may not be correctly reproduced by 2×2 matrix ensembles, which have a nongeneric distribution of branch points.

For the case of stationary ensembles, we have shown numerically that, whereas the Fourier amplitudes a_n of the eigenvalues are approximately Gaussian distributed when n is small in comparison to the width of the Fourier spectrum, strong deviations from Gaussian distribution occur at large n. This behavior can be qualitatively connected with the statistical distribution of level derivatives, which have Fourier expansions in which the role of the non-Gaussian amplitudes a_n is enhanced, the more, the higher the order of the derivative. While first-order derivatives (level velocities) are still Gaussian distributed, this is no longer true already for second-order derivatives

(level curvatures), which have, in fact, a generalized Cauchy distribution; a strongly non-Gaussian distribution is, therefore, to be expected for all higher-order derivatives.

Our theoretical apparatus heavily hinges on periodicity, and it is a natural question, whether any of our conclusions can be generalized to the general case of a nonperiodic parameter dependence. Some kind of a stationary behavior is needed in order that a velocity correlation may be defined; an essential step is then to filter out any "secular" component of the eigenvalue motion, as can be done, e.g., by the unfolding process. In any case, the resulting branch-point pattern and the corresponding Fourier analysis may be, in our opinion, significantly different from the periodic case discussed in this paper.

APPENDIX

We compute analytically the velocity correlation for the level dynamics of 2×2 matrices $H(\varphi) = H_1 \cos\varphi + H_2 \sin\varphi$, where

$$H_1 = \begin{bmatrix} a_1 & \frac{1}{\sqrt{2}}(x_2 + ix_3) \\ \frac{1}{\sqrt{2}}(x_2 - ix_3) & a_2 \end{bmatrix} ,$$

$$H_2 = \begin{bmatrix} b_1 & \frac{1}{\sqrt{2}}(y_2 + iy_3) \\ \frac{1}{\sqrt{2}}(y_2 - iy_3) & b_2 \end{bmatrix} \tag{A1}$$

both belonging to GUE or GOE; in the latter case $x_3 = y_3 = 0$. All matrix elements are normally distributed with the same variance. Setting $a_1 + a_2 = \sqrt{2}a$, $b_1 + b_2 = \sqrt{2}b$, $a_1 - a_2 = \sqrt{2}x_1$, and $b_1 - b_2 = \sqrt{2}y_1$, we have the following expressions for the eigenvalues:

$$e_\pm(\varphi) = \frac{1}{\sqrt{2}}(a\cos\varphi + b\sin\varphi) \pm \frac{1}{\sqrt{2}}|\vec{x}\cos\varphi - \vec{y}\sin\varphi| . \tag{A2}$$

We begin by computing the following eigenvalue correlator, which actually depends on the difference $\varphi = \varphi_2 - \varphi_1$:

$$F(\varphi) = \left[\frac{\omega}{\pi}\right]^{n+1} \int da \, db \, d^n x \, d^n y \, e^{-\omega(a^2 + b^2 + |x|^2 + |y|^2)}$$

$$\times \tfrac{1}{2}[e_+(\varphi_1)e_+(\varphi_2) + e_-(\varphi_1)e_-(\varphi_2)] \tag{A3}$$

with $n = 2, 3$, respectively, for GOE and GUE. The velocity correlator is then obtained as a second derivative: $C(\varphi) = -F''(\varphi)\Delta^{-2}$.

The eigenvalue correlator is the sum of two contributions $F_1 + F_2$, where

$$F_1 = \frac{\omega}{\pi} \int da \, db \, e^{-\omega(a^2 + b^2)} \tfrac{1}{2}(a\cos\varphi_1 + b\sin\varphi_1)$$

$$\times (a\cos\varphi_2 + b\sin\varphi_2) = \frac{1}{4\omega}\cos\varphi ,$$

$$F_2 = \left[\frac{\omega}{\pi}\right]^n \int d^n x \, d^n y \, e^{-\omega(|x|^2 + |y|^2)} \tfrac{1}{2}|\vec{x}\cos\varphi_1 - \vec{y}\sin\varphi_1|$$

$$\times |\vec{x}\cos\varphi_2 - \vec{y}\sin\varphi_2| .$$

With the linear change of variables, for φ different from 0 and $\pm\pi$,

$$\vec{u} = \frac{\sqrt{\omega}}{\sin\varphi}(\vec{x}\cos\varphi_1 - \vec{y}\sin\varphi_1) ,$$

$$\vec{v} = \frac{\sqrt{\omega}}{\sin\varphi}(\vec{x}\cos\varphi_2 - \vec{y}\sin\varphi_2)$$

the second integral simplifies to

$$F_2 = \frac{1}{2\pi^n\omega}|\sin\varphi|^{n+2} \int d^n u \, |u|$$

$$\times \int d^n v \, |v| e^{-|u|^2 - |v|^2 + 2\vec{u}\cdot\vec{v}\cos\varphi} . \tag{A4}$$

Note that F_2 is an even function of φ.

Let us first consider the case of GOE. In polar coordinates, letting θ be the angle between the two vectors $\vec{u}$ and $\vec{v}$, we have

$$F_2(\varphi) = \frac{1}{2\pi^2\omega}\sin^4(\varphi)2\pi \int_0^\infty u^2 du \int_0^\infty v^2 dv \, e^{-u^2 - v^2}$$

$$\times \int_0^{2\pi} d\theta \, e^{2uv\cos\varphi\cos\theta}$$

$$= \frac{2}{\omega}\sin^4(\varphi) \int_0^\infty u^2 du \int_0^\infty v^2 dv \, e^{-u^2 - v^2}$$

$$\times I_0(2uv\cos\varphi) , \tag{A5}$$

where $I_0(x)$ is a Bessel function. The double integral is tabulated and we obtain

$$F_2(\varphi) = \frac{1}{4\omega}[2E(\cos\varphi) - \sin^2(\varphi)K(\cos\varphi)] ,$$

where E and K are the complete elliptic functions. Adding the F_1 term and computing the second derivative we get the velocity correlator for GOE. Explicitly, it is a function of $t = \cos\varphi$,

$$\frac{C(\varphi)}{C(0)} = \frac{1}{2t^2}[t^3 + E(t) - (1 - t^4)K(t)] . \tag{A6}$$

The small φ expansion has the expected logarithmic term;

$$\frac{C(\varphi)}{C(0)} = 1 - \varphi^2(\tfrac{3}{2}\ln 2 - \tfrac{1}{8} - \tfrac{3}{4}\ln|\varphi|) + O(\varphi^4) \; . \qquad \text{(A7)}$$

At $\varphi = \pi/2$ ($t = 0$), the normalized correlator has the value $-\pi/8$, and at $\varphi = \pi - \epsilon$ it vanishes as $-\epsilon^2[(1/8) + (3/4)\ln(4/\epsilon)]$.

Let us now consider the GUE case. In spherical coordinates, letting θ be the angle between the vectors $\vec{u}$ and $\vec{v}$, we have

$$F_2(\varphi) = \frac{1}{2\pi^3\omega} |\sin\varphi|^5 8\pi^2 \int_0^\infty u^3 du \int_0^\infty v^3 dv \, e^{-u^2 - v^2}$$

$$\times \int_0^\pi d\theta \, \sin(\theta) e^{2uv\cos\varphi\cos\theta}$$

$$= \frac{1}{\pi\omega} \frac{|\sin\varphi|^5}{\cos\varphi} \int_0^\infty du \int_0^\infty dv \sqrt{uv} \, e^{-u-v}$$

$$\times \sinh(2\sqrt{uv}\cos\varphi) \; . \qquad \text{(A8)}$$

The double integral can be related to the following, available in the tables ($pq > 1/4$):

$$\int_0^\infty dx \int_0^\infty dy \, \cosh(\sqrt{xy}) e^{-px - qy}$$

$$= \frac{4}{4pq - 1} + \frac{4}{(4pq - 1)^{3/2}} \arcsin\left[\frac{1}{2\sqrt{pq}}\right] \; .$$

For $0 < \varphi < \pi$ the result is

$$F_2(\varphi) = \frac{1}{2\pi\omega} \left[\left|\frac{\pi}{2} - \varphi\right| \left(3\cos\varphi + \frac{\sin^2\varphi}{\cos\varphi}\right) + 3\sin\varphi \right] \; .$$

After summation of the F_1 term and derivating twice we obtain the velocity correlation for 2×2 GUE matrices,

$$\frac{C(\varphi)}{C(0)} = \left[\frac{3}{2} - 2\frac{\varphi}{\pi}\right] \cos\varphi$$

$$+ \frac{1}{\pi} \left[\frac{1}{\cos\varphi} - \frac{2}{\cos^3\varphi}\right] \left[\frac{\pi}{2} - \varphi - \frac{1}{2}\sin(2\varphi)\right] \; . \qquad \text{(A9)}$$

In particular, we compute the following Mac Laurin expansion:

$$\frac{C(\varphi)}{C(0)} = 1 - 2\varphi^2 + \frac{16}{3\pi}|\varphi|^3 + O(\varphi^4) \; . \qquad \text{(A10)}$$

At $\varphi = \pi/2$ the function takes the value $-4/(3\pi)$ and vanishes as $-(3/2)\epsilon^2$ for $\varphi = \pi - \epsilon$.

[1] M. L. Mehta, *Random Matrices* (Academic, New York, 1991).

[2] L. P. Gorkov and G. M. Eliashberg, Zh. Eksp. Teor. Fiz. **48**, 1407 (1965) [Sov. Phys. JETP **21**, 940 (1965)].

[3] K. B. Efetov, Adv. Phys. **32**, 53 (1983).

[4] B. L. Altshuler and B. I. Shklovskii, Zh. Eksp. Teor. Fiz. **91**, 220 (1986) [Sov. Phys. JETP **64**, 127 (1986)].

[5] A. Szafer and B. L. Altshuler, Phys. Rev. Lett. **70**, 587 (1993).

[6] C. W. Beenakker, Phys. Rev. Lett. **70**, 4126 (1993).

[7] B. D. Simons, A. Szafer, and B. L. Altshuler, Pis'ma Zh. Eksp. Teor. Fiz. **57**, 276 (1993) [Sov. Phys. JETP Lett. **57**, 268 (1993)]; B. D. Simons and B. L. Altshuler, Phys. Rev. Lett. **70**, 4063 (1993); Phys. Rev. B **48**, 5422 (1993); M. Faas, B. D. Simons, X. Zotos, and B. L. Altshuler, *ibid.* **48**, 5439 (1993); B. D. Simons, P. A. Lee, and B. L. Altshuler, *ibid.* **48**, 11450 (1993).

[8] G. Casati, I. Guarneri, F. Izrailev, L. Molinari, and K. Życzkowski, Phys. Rev. Lett. **72**, 2697 (1994).

[9] K. Życzkowski, F. Izrailev, and L. Molinari, J. Phys. (France) I **4**, 1469 (1994).

[10] D. Braun and G. Montambaux, Phys. Rev. B **50**, 7776 (1994).

[11] U. Sivan, F. P. Milliken, K. Milkove, S. Rishton, Y. Lee, J. M. Hong, V. Boegli, D. Kern, and M. deFraza, Europhys. Lett. **25**, 605 (1994).

[12] F. Haake, *Quantum Signatures of Chaos* (Springer, Berlin, 1991).

[13] P. Gaspard, S. A. Rice, and K. Nakamura, Phys. Rev. Lett. **63**, 930 (1989); P. Gaspard, S. A. Rice, H. J. Mikeska, and K. Nakamura, Phys. Rev. A **42**, 4015 (1990).

[14] D. Saher, F. Haake, and P. Gaspard, Phys. Rev. A **44**, 7841 (1991).

[15] J. Zakrzewski and D. Delande, Phys. Rev. E **47**, 1650 (1993).

[16] J. Zakrzewski, Z. Physik B (to be published).

[17] M. V. Berry and J. P. Keating, J. Phys. A **27**, 6167 (1994).

[18] W. D. Heiss and W. H. Steeb, J. Math. Phys. **32**, 3003 (1991).

[19] J. D. Murray, *Asymptotic Analysis* (Clarendon, Oxford, 1974).

[20] M. F. Neuts, *Probability* (Allyn and Bacon, Boston, 1973), p. 244.

[21] M. F. Neuts, *Probability* (Ref. [20]) p. 261.

[22] M. Wilkinson, J. Phys. A **22**, 2795 (1989).

[23] J. Zakrzewski and M. Kuś, Phys. Rev. Lett. **67**, 2749 (1991).

[24] J. Zakrzewski, D. Delande, and M. Kuś, Phys. Rev. E **47**, 1665 (1993).

[25] F. von Oppen, Phys. Rev. Lett. **73**, 798 (1994).

[26] Y. Fyodorov and H. J. Sommers (unpublished).

[27] E. Akkermans and G. Montambaux, Phys. Rev. Lett. **68**, 642 (1992).

[28] B. D. Fried and S. D. Conte, *The Plasma Dispersion Function* (Academic, New York, 1961).

[29] J. Spanier and K. B. Oldham, *An Atlas of Functions* (Emisphere, Washington, 1987).

[30] A. Pandey and M. L. Mehta, Commun. Math. Phys. **16**, 2655 (1983).

[31] A. Kamenev and D. Braun, J. Phys. (France) I **4**, 1049 (1994).

[32] N. Taniguchi, A. Hashimoto, B. D. Simons, and B. L. Altshuler, Europhys. Lett. **27**, 335 (1994).

[33] Although crossing of different eigenvalues at real values of

φ is possible, such real crossings would not spoil the analyticity of $e(\varphi)$.

[34] In fact, in the GUE and GSE cases the asymptotic behavior of $\langle |a_n|^2 \rangle$ entails that the series for K is mean-square convergent, so that a Gaussian distribution of all terms in the series would enforce a Gaussian distribution of its sum.

[35] The value of w^* can also be estimated from the large φ behavior, Eq. (39) of Ref. [17]; a much larger value is found in this way. Though the large φ behavior is now correct, the small and intermediate φ behavior is in even stronger disagreement with numerical data.

[36] We note in passing that this singularity is an integrable one, and that this fact alone is sufficient to exclude that the second derivative of $C(\varphi)$ may be singular at $\varphi=0$: see the remarks following Eq. (2.20).